DELFT UNIVERSITY OF TECHNOLOGY

REPORT 10-06

Flow estimation for the Persian Gulf using a Kelvin wave expansion

M.A. Badri, P. Wilders & A.R. Azimian

ISSN 1389-6520

Reports of the Department of Applied Mathematics

Delft 2010

Flow estimation for the Persian Gulf using a Kelvin wave expansion

M.A. Badri[1]

Subsea R&D center, Isfahan University of Technology, Iran
E-mail: malbdr@cc.iut.ac.ir

P. Wilders[2]
Dept. of Electrical Eng., Math. and Comp. Sc., Delft University of Technology, The Netherlands
E-mail: p.wilders@tudelft.nl

A.R. Azimian[3]
Dept. of Mechanical Eng., Isfahan University of Technology, Iran
E-mail: azimian@cc.iut.ac.ir

Abstract

Hydrodynamic simulations of tidal currents in the Persian Gulf are presented. Water surface level and velocity have been determined by a Kelvin wave expansion as a new hydrodynamic calibration tool for estimating the dynamical field and flow patterns. In the procedure, leading to the Kelvin wave expansion, data of tidal constituents from co-tidal charts play a role. Results of the simplified model have been compared with both measurements as well with the results of a full reference hydrodynamic model to reveal that this calibration approach is a promotion not only towards simplicity, but also towards a speed up of the computation. Also a short-term oil spill simulation was undertaken. Comparison of the actual and simulated oil spill drift was found acceptable, allowing for future application in risk assessment analysis in the northern part of the Iranian waters.

Keywords: Shallow water equations, Flow estimation, Kelvin wave expansion, Tidal constituents, Oil spill model, Persian Gulf

1. Introduction

1. Assistant Professor
2. Professor
3. Professor

With respect to oil, the Persian Gulf and its surroundings play a prominent role. An issue, that needs to be addressed to, is oil damage. Several aspects can be considered. Among others, it might be of some importance to have access to a global and computational efficient tool for a quick analysis of the movement of oil spills during the first couple of days. In this case, not all residual currents need to be taken into account, enabling the application of an approximate flow model.

Several detailed oil spill studies of the Persian Gulf have become available in the past 15 years, e.g. El-Sabh and Murty (1988), Al-Rabeh et al. (1992), Venkatesh and Murty (1994), Sabbagh-Yazdi (2006), Elhakeem et al. (2007). All of these studies employ advances and computational expensive flow models. In this paper, an alternative at this point is put forward by formulating an approximate flow model using the well known Kelvin waves. The resulting model is highly efficient. Of course, the model is global of nature and can not be used for very detailed studies.

The hypothesis in the present work is that the main tidal motion in the Persian Gulf is due to Kelvin waves, e.g. Venkatesh and Murty (1994), Blair (2000), and that it must be possible to provide an approximate flow model valid for periods of about 10 days by considering an appropriate Kelvin wave expansion. This paper provides such an expansion and the performance of this expansion is studied in some details.

Capturing the main tidal motion using simplified techniques is a field of ongoing activity. In Marinone et al. (2009) a web portal has been made available for describing tidal movement in the Gulf of California using a straightforward 14-component tidal Fourier expansion with coefficients extracted from a database generated using a 3D hydrostatic numerical model. A similar approach is followed by Ommundsen (2002), using few Fourier components and this enables the author to capture the main tidal movement in the Vestfjorden Area. Yanagi and Takao (1998) carry out a study, showing that a model with a simple and approximate geometry enables to capture the main tidal characteristics of the Gulf of Thailand.

This paper is organized as follows: In section 2 some of the main characteristics of the Persian Gulf are described and section 3 gives a brief account on Kelvin waves. The underlying wave phenomenon is well known and has been studied over the last decades. Section 4 presents the Kelvin wave expansion adopted in this study. In this expansion we

focus on the main tidal constituents, i.e. M_2, S_2, K_1 and O_1. For determining the coefficients in the expansion a fit to the data, such as provided by the admiralty tables, has been introduced. For reasons of comparison, a more elaborated flow model has been developed as well and is described in section 5. In this section, it is also shown that the resulting MIKE3-HD model may serve as a reference model in the present study. This paper is devoted to flow modeling. However, all efforts are done against the background of oil spill modeling. As a consequence, the final proof of the validity of the present approach needs to be found in the area of oil spill modeling. In order to be able to include a small example related to oil spill modeling as well, we present a short overview of our spill model in section 6. Section 7 discusses the results. The Kelvin wave expansion is compared both with measurements as well as with the MIKE3-HD reference model. Good results are obtained, showing that the Kelvin wave expansion has some intrinsically good features and performs quite well. Also the Habash oil spill is discussed in section 7. Simulations using both the Kelvin wave expansion as well as the MIKE3-HD reference model are performed and compared with actual data. It can be observed that taking the flow data from the Kelvin wave expansion enables a good simulation of this spill for the first couple of days. Finally, in section 8 some conclusions are presented and a brief discussion on future work takes place.

2. Persian Gulf characteristics

The Persian Gulf, in the southwest Asian region, is an extension of the Indian Ocean located between Iran and the Arabian Peninsula. It lies entirely north of the tropic of Cancer and so is strictly subtropical. The Persian Gulf, located between 24° and 30° latitude is about 1,000 km in length along its main axis. It is a semi-enclosed sea, varying in width from a maximum of 340 km to a minimum of 60 km in the Strait of Hormuz. This basin is entirely located on a shallow continental platform, rarely deeper than 100 m with a mean depth of about 35 m, which at the Strait of Hormuz connects directly with the great depths of the Gulf of Oman by a steep continental slope. The important topographic features are the deeper water near the Iranian coast and the shallow areas in the southwestern parts.

A vast area of the Persian Gulf is considered as a shallow water basin. Usually, the kh parameter is introduced to measure the depth strength; k is the wave number and h the mean depth. By means of the shallow water definition $kh < 0.7$ (Komen et al. (1995)), it is revealed that the Persian Gulf meets the condition of shallow water. Because of this shallowness of the Persian Gulf, several numerical workers have applied the set of shallow water continuity and momentum equations for simulation of tidal currents in the Persian Gulf.

The oceanography of the Persian Gulf is such that it is an almost isolated system, except for the tide entering from the Gulf of Oman through the Strait of Hormuz as an open boundary. The resulting tidal motion consists of a variety of tidal types with higher amplitudes occuring in the Strait of Hormuz. Analysis of tidal heights from numerous coastal stations around the Gulf has, in Admiralty (1996), led to the publication of comprehensive charts of co-amplitudes and co-phase lines for the principal constituents M_2, S_2, K_1 and O_1 which are used here.

3. Kelvin waves

Consider a long straight coast line $y = 0$ in the northern hemisphere with water at its left side and a simple wave traveling along this boundary. Due to the rotation of the earth, the water level builds up at the coast, which results in a greater wave amplitude nearer the coast. This leads to a pressure gradient which balances the rotational force. The wave resulting from this is called a Kelvin wave, e.g. Pedlosky (1987). Kelvin waves are special solutions of the small amplitude frictionless linearized inviscid depth-averaged shallow water equations, i.e.

$$\frac{\partial \eta}{\partial t} + \frac{\partial (uH)}{\partial x} + \frac{\partial (Hv)}{\partial y} = 0, \quad -\infty < x < \infty, y > 0 , \tag{1}$$

$$\frac{\partial u}{\partial t} - f v = - g \frac{\partial \eta}{\partial x} , \tag{2}$$

$$\frac{\partial v}{\partial t} + f u = - g \frac{\partial \eta}{\partial y} , \tag{3}$$

satisfying the boundary condition

$$v = 0 \text{ at } y = 0 . \tag{4}$$

It also satisfies the condition that the wave amplitude is decaying away from the coast. In relations (1), (2), (3), η denotes the surface elevation with respect to the reference plane, u and v are the horizontal depth-averaged velocity components, H is the constant averaged depth, f is Coriolis factor and g is the acceleration of gravity. In order to determine the Kelvin wave, one may consider the trial solution.

$$\eta = f_1(y)e^{\pm i(kx-\sigma t)} , u = f_2(y)e^{\pm i(kx-\sigma t)} , v = f_3(y)e^{i(kx-\sigma t)} . \tag{5}$$

The functions f_1, f_2, f_3 are determined such that this trial solution solves the differential equations and satisfies the conditions put forward. Some lengthy computations show that $f_1, f_2, f_3 \propto e^{-\beta y}$, with algebraic equations for the parameters implying $f_3 = 0, \sigma^2 = C^2k^2, \beta = f/C$, where $C = \sqrt{gH}$. As a result, the Kelvin wave, written in its most compact form, reads:

$$\eta = \eta_0 e^{-\frac{f}{C}y} cos[k(x \pm Ct) + \varphi], \quad u = \frac{C}{H}\eta, \quad v = 0 . \tag{6}$$

For a Rossby radius $R = C/f$ from the coast line ($y = 0$), the amplitude has fallen to $0.37\eta_0$, Pugh (1996). In practice, Kelvin waves are most important for describing tidal amplitudes in presence of long coastlines. The tidal movement in the Persian Gulf near the Iranian coast stems mainly from Kelvin waves traveling inward from the Strait of Hormuz along the northeast coast. Figure 1 presents the approximate setting, taken by us, to describe the Kelvin wave. In fact, the plane of the domain is rotated under an angle of $\theta = 25.9^\circ$ in order to fit the domain to the new coordinate system (x', y') , making the coastline nearly parallel to coordinate lines. The mode from (6), traveling inwards, reads:

$$\eta = \eta_0 \, e^{-\frac{f}{C}y'} \cos[k(x' - Ct) + \varphi], \quad u' = \frac{C}{H}\eta, \quad v' = 0 \,. \tag{7}$$

Here, x', y' are coordinates in a rotated frame (Figure 1) and u', v' are the velocity components with respect to the rotated frame. To accomplish expressions in the $x, y-$coordinate system it needs to be observed that:

$$\begin{bmatrix} x \\ y \end{bmatrix} = M \begin{bmatrix} x' \\ y' \end{bmatrix}, \quad \begin{bmatrix} u \\ v \end{bmatrix} = M \begin{bmatrix} u' \\ v' = 0 \end{bmatrix}, \quad M = \begin{bmatrix} \cos\theta & \sin\theta \\ -\sin\theta & \cos\theta \end{bmatrix} \tag{8}$$

4. Kelvin wave expansions

It is well-known that the main constituents for tidal motion are the principal semi-diurnal lunar and solar tides M_2, S_2 and the principal diurnal tides K_1, O_1. In particular, it is known that the waves entering the Persian Gulf at the Strait of Hurmoz will carry the associated frequencies of which the data are given in Table 1 for each constituent**.** In this table T and $k = 2\pi/\lambda = 2\pi/(T\sqrt{gH})$ are the period and the wave number respectively, assuming a typical depth of 35 m (see section 2).

We number the four main constituents with $j = 1, 2, 3, 4$. Here, $j = 1$ corresponds with M_2, $j = 2$ with S_2, $j = 3$ with K_1 and $j = 4$ with O_1. All four constituents introduce a Kelvin wave, traveling into the Persian Gulf with elevation:

$$\eta_j = \eta_{0j} \, e^{-\frac{f}{C}y'} \cos[k_j(x' - Ct) + \varphi_j] \,. \tag{9}$$

Taking all four together we obtain as an approximate flow model the following Kelvin wave expansion:

$$\eta = Z_0 + \sum_{j=1}^{4} \eta_j \,, \quad u' = \frac{C}{h} \sum_{j=1}^{4} \eta_j \,, \quad v' = 0 \,. \tag{10}$$

It must be remarked that the typical depth parameter H, occurring in earlier formulae has everywhere, been replaced by the still-water depth h in order to obtain (10). Among

others, this means that in (9) and (10) the wave speed C and wave number k are spatially dependent. The bathymetry has been provided to us by the Iranian Hydrographic Center.

Basic data concerning tidal flow in the Persian Gulf can be obtained from Admiralty (1969). The admiralty tables contain charts of co-amplitude and co-phase lines based on time averaged field data for each constituent. It is our intention to use these data for establishing the unknown coefficients in (10). Let us denote the amplitude and phase taken from these tables with μ_j and θ_j respectively. As an example, Table 2 presents the amplitudes and phases for a grid point close to Kish Island.

To give an impression on the consistency of the data used, we have compared the data from the admiralty tables with data on amplitudes and phases, such as presented to us by the Iranian Hydrographic Center, at four reference locations, i.e. Kish and Siri Islands, Bandar Abbas and Bushehr Port. Table 3 results from this. In this table the maximal and minimal deviations over the four locations are presented. The agreement between the two is reasonable.

Starting from μ_j it is possible to define normalized values $\tilde{\mu}_j$. Here, normalization is done with respect to coastal amplitudes. In fact,

$$\tilde{\mu}_j = \mu_j \Big/ \sum_{j=1}^{4} \mu_{j_0} \ , \tag{11}$$

with μ_{j_0} referring to coastal amplitudes taken at related coastline positions according to the basic definitions. To obtain this position it is just needed to determine the present position in the (x', y') coordinate system, next traveling towards the coast keeping x' equal.

Let us now return to (10). The mean surface level Z_0, has been determined using the following relation

$$Z_0 = 0.15 + \sum_{j=1}^{4} \mu_j \ . \tag{12}$$

This relation, valid for the Persian Gulf, concerns the mean sea level and stems from the Iranian Hydrographic Center. Basically, (12) originates from the admiralty tables, where they have added the value 0.15 to account for seasonal streams. Here, calibration has been done by this Center using about 20 years of field data.

Consulting (9) and (10), it can be seen that it remains to specify the coefficients η_{0j} and φ_j. In fact, we took

$$\eta_{0j} = \tilde{\mu}_j \ , \varphi_j = \theta_j \ . \tag{13}$$

The choice (13) resulted from a trial and error procedure and showed up to be the best.

Using the charts from the admiralty table, we have determined the amplitudes and phases of each of the main constituents in the grid points of the $0.25^\circ \times 0.25^\circ$ coarse grid. The coarse grid is much coarser than grids used for computational reasons later on. These grids are in general obtained by refinement of the coarse grid and in order to obtain η_{0j} and φ_j on the fine grid as well, a simple bilinear interpolation is employed. For completeness of the procedure, it is necessary to present values of η_{0j} and φ_j in some of the land points of the coarse grid and we have just taken zero values for this aim. This implies that our procedure, very close to the boundaries is not accurate. However, against the background of the more global character of the present study, this was found acceptable.

5. A full hydrodynamic model

For reasons of comparison, a full hydrodynamic model, based on the software package MIKE3 (2002), is considered as well. In the present study, the 3D non-hydrostatic $z-$layer version of the MIKE3-HD software has been used in combination with $k-\varepsilon$ closure. Here, developments are in line with Elhakeem et al. (2007). However, these authors include a more extended physical model taking salinity and temperature effects into account.

At Hurmoz strait there is an open boundary with prescribed surface elevation fluctuation. Field data at Didamar Island have been obtained from the Iranian

Hydrographic Center, see Figure 2. The corresponding elevation has been superimposed at the full boundary. Further boundaries are assumed to be coastal and thus closed with zero normal velocity components. Islands are included in the MIKE3-HD runs.

As has been outlined before, the considered geometry and bathymetry of the Persian Gulf has been provided to us by the Iranian Hydrographic Center. The prevailing wind direction in the Persian Gulf is from NW to SE. The wind field imposed, consists of a yearly-averaged field, provided by the Iranian bureau of Oceanography and Meteorology and has a velocity with magnitude 5.25 [m/sec] and direction 315°.

The horizontal unstructured grid has 13532 elements with a typical spatial grid size of 5490×4575 [m], which is $3' \times 2.5'$. Later on, this grid and the associated MIKE flow field is used also in the particle-based oil spill model. In the oil spill model we impose the constraint that a particle must not move more than one grid cell in each time step in order to make the computations stable. Therefore, we have asked MIKE to provide the flow data every 30 [min]. In MIKE, further time stepping procedures are carried out automatically.

To verify the full hydrodynamic model, computed values for water surface level and surface layer currents near Kish Island have been compared with measured data from the Iranian Hydrographic Center. Figure 3 compares the water surface level for the 12-days time interval 25 April–6 May 2007. It can be seen that the MIKE3-HD model needs to warm up. After that the agreement is acceptable. The comparison period was chosen based on the actual available measured data from a current meter at the depth of 10 m near Kish Island. Comparison of the averaged surface layer currents is done in Figure 4 and shows a fair agreement between measurement data and predicted results obtained from the full hydrodynamic model. From these comparisons it may be concluded that the MIKE3-HD model is suitable for reference purposes in the present study. It is interesting to relate the present comparison to others available in literature. Elshorbagy et al. (2006) compare, on basis of the so-called multilevel numerical model, both water levels and currents at two measurements stations along the Iranian coast. Also here, only the main trend is captured for the currents. In Elhakeem et al. (2007) currents and water levels are compared for a station not too far from Kish Island, with computations carried out on basis of an alternative MIKE3-HD model. In this publication the comparison for the

current seems to be a little more favorable than elsewhere, but again only the main trend is captured.

6. Oil spill model

In order to be able to include a small example of an oil spill, we pay some attention to the oil spill model. The model is a quite complete in-house model of which the details are presented in Badri et al. (2010a), Badri et al. (2010b). Here we only discuss its main characteristics. The oil spill model is a 3D particle model collecting known formulations for oil drop emergency, surface oil spill spreading, vertical dispersion, evaporation and emulsification. At the mathematical basis of the model, we find the stochastic differential equation formulation of advection-dispersion with centered Gaussian distributions to model dispersion. The basic ideas have been presented at many places, e.g**.** Venkatesh (1988), Al-Rabeh et al. (1989), Wang et al. (2005)**.** Although, it is possible to establish stochastic formulations of dispersion using uniform distributions, which is often done in older literature, our preference is in favor of the more modern formulation using Gaussian (normal) distribution, e.g. Lonin (1999), Korotenko et al. (2000). It is well-known that oil spill models contain several empirical parameters. As far as necessary, parameters have been calibrated for application in the Persian Gulf. The oil spill model is 3D and needs the vertical velocity profile of the flow. In the full hydrodynamic model, presented in section 5, this profile is automatically available. However, the approximate flow model, presented in section 4, models the surface velocities only. This model is extended assuming a classical logarithmic profile for the vertical velocity.

The final velocity determining the advection is composed of the flow velocities and the wind-induced velocities. Let $\vec{u} = [u,v]^T$ denote the horizontal velocity vector at the surface, then

$$\vec{u} = \vec{u}_{flow} + k_w(z)\vec{u}_{wind} \ . \tag{14}$$

Here, $\vec{u}_{flow}$ is the velocity vector resulting from the flow model and $\vec{u}_{wind}$ is the wind velocity at 10 meters above the sea level. The function $k_w(z)$ determines the drift resulting from the wind. It is common to use:

$$k_w(z) = k_w^* (1-3\frac{z}{H})(1-\frac{z}{H}), \quad 0 \le z \le H \ . \tag{15}$$

Here, k_w^* is the wind drift factor, H is the local water depth and z is the vertical coordinate of the particle along the line reaching from $z = 0$ at the surface to $z = H$ at the bottom. In case studies by MIKE3-HD, it has been observed that the wind contribution to the flow is in the same direction as the wind in the upper third of the water column and in the opposite direction in the remaining lower part of the water column and the present formula is in full agreement with this. The influence of wind on oil spills is significant and, therefore, some caution is needed here. The wind field at 10 meters above sea level, necessary for oil spill modeling, has been determined in quite an advanced manner using analytical wind fields tuned to measurements, see Badri et al. (2010b) for details.

The total volume of the spilled oil on the sea surface has been characterized by the number N of infinitesimal particles under the influence of the regular movement of the medium. Spatial fluctuations can be calculated based on the random walk technique and the coordinates X_k, Y_k and Z_k of the kth particle, moving away from X_k^0, Y_k^0, Z_k^0 during a time step Δt, are determined by:

$$X_k = X_k^0 + u\,\Delta t + [W_1]_{\mu=0}^{\sigma^2=1} \sqrt{2D_h\,\Delta t} \ , \tag{16}$$

$$Y_k = Y_k^0 + v\,\Delta t + [W_2]_{\mu=0}^{\sigma^2=1} \sqrt{2D_h\,\Delta t} \ , \tag{17}$$

$$Z_k = Z_k^0 + (w + w_b)\,\Delta t + [W_3]_{\mu=0}^{\sigma^2=1} \sqrt{2D_v\,\Delta t} \ . \tag{18}$$

The velocity components u, v and w are determined either using the dynamical field resulting from the Kelvin wave expansion or by applying the full MIKE3-HD model.

$[W_1]_{\mu=0}^{\sigma^2=1}$, $[W_2]_{\mu=0}^{\sigma^2=1}$ and $[W_3]_{\mu=0}^{\sigma^2=1}$ are three independent random variables following reduced centered Gaussian distributions (i.e. with zero average and variance 1). D_h and D_v are the horizontal and vertical dispersion coefficients. The term containing w_b is a consequence of oil drop emergence and we basically follow Zheng et al. (2000) to model this term.

7. Results

The dynamical field has been obtained by two different hydrodynamic models. The first uses the Kelvin wave expansion and the second is the full MIKE3-HD model. In this section we evaluate both.

In a first step, the focus is on amphidromic points. It is worth mentioning that an amphidromic point is a point where the tidal fluctuation is almost zero and its occurrence hinges on the interference between Coriolis effects and bathymetry. Figure 5 shows the water surface fluctuations generated by the Kelvin wave expansion at amphidromic points for the K_1, O_1 constituents. A maximum elevation of 5 [cm] is seen, which is small compared to the maximum tidal water level elevation (of the order of 4 [m], as documented by Rakha et al. (2007)). Thus the Kelvin wave expansion performs well as far as it concerns amphidromic points, which is due to the fact that basic coefficients are picked up from field data. It might be that extending the Kelvin wave expansion with extra terms, containing reflected Kelvin waves, may help to improve the performance at the amphidromic points. This would be a possible subject of future research.

Let us consider Figure 2 again. It presents the water elevation at Didamar Island/Hormuz strait, such as provided by the Iranian Hydrographic Center. In Figure 6 these data as well as the results of the Kelvin wave expansion have been plotted. It can be seen that the comparison is reasonable. The Figures 7 and 8 show the measured data near Kish Island and the computed values using the Kelvin wave expansion. A good agreement can be observed.

The two hydrodynamic models are compared in Figures 9 and 10 with regard to water surface level and water surface velocity. In the first half of the time interval, the

hydrodynamic model MIKE3-HD is in its warming-up period. As shown, the water elevations are in good agreement in the second half of the time interval. With respect to the velocity, the two time series follow each other. In Figure 11 measured and computed water surface velocities for the two hydrodynamic models are compared with each other over the whole interval. The time index is referred to as 192 data points coming from 16 days with two hours intervals. It shows that the mean deviation between measured and computed water surface velocity is about 18 per cent better for the Kelvin wave expansion than for the full MIKE3-HD hydrodynamic model. Moreover, CPU time for the MIKE3-HD was found to be about 4–8 hours per run based on the simplest conditions in comparison with 2 minutes for the Kelvin wave expansion, which presents a successful speed-up.

Next, a short investigation is done of the oil spill model for the Habash oil spill event. Figure 12 shows the location of the oil slick on the grid in the $(x,y)-$plane for a period of approximately 1.5 days, applying both hydrodynamic models. As can be seen, the locations are almost the same and the maximal deviation is about one grid length after approximately 1.5 days. Figure 13 shows the oil slick trajectory for a period of approximately one week using the Kelvin wave expansion. The figure shows also the actual data for the Habash oil spill event and computed results based on the GULFSLIK model, both taken from El-Sabh and Murty (1988). A fair agreement can be observed.

8. Conclusion

A flow estimation model to generate the dynamical field in the Persian Gulf has been presented. The model shows how the geostrophic approximation can be systematically exploited to produce a dynamical framework adequate for the calculation of motions. The model incorporates the essential dynamical character of the geophysical system and has its roots in Kelvin wave theory. It has been revealed that this new hydrodynamic calibration approach presents an alternative for the more of the used numerical hydrodynamic models, such as MIKE3-HD. The improvement is not only towards an estimation of the flow pattern in a simple manner, but also shows a successful speed-up.

The model is used for an application involving the prediction of the trajectory of spilled oil on the short term. Also here, the new model shows a good performance. In the present work we have included only a small example illustrating this. In future work more details will be added. The final outcome will be that we have established a simple estimation procedure for the flow pattern that enables us to speed up the computations significantly. With such a speedy procedure available it is possible to determine a large number of predictive results in the context of risk assessment studies. In this manner we hope to be able to provide oil spill hazard contour maps in the future.

References

Admiralty Manual of Hydrographic Surveying, Chapter 1: Tides and Tidal Streams, Volume 2 N.P.134b (2), 1969, Hydrographer of the Navy, Taunton, Somerset, HMSO press, Edinburgh, UK.

Al-Rabeh, A.H., Cekirge, H.M., Gunay, N., 1989, A stochastic simulation model of oil spill fate and transport, Applied Mathematics Modelling 13, 322-329.

Al-Rabeh, A.H., Cekirge, H.M., Gunay, N., 1992, Modeling the fate and transportation of Al-Ahmadi oil spill, Water, Air and Soil Pollution 65, 257-279.

Badri, M.A., Azimian, A.R., 2010a, An oil spill model based on the Kelvin wave theory and artificial wind field for the Persian Gulf, Indian Journal of Marine Sciences, to be published.

Badri, M.A., Wilders, P., Azimian, A.R., 2010b, Oil spill simulation for the Persian Gulf based on a new and efficient flow estimation procedure, Report 10-07. Department of Mathematics, Delft University of Technology, The Netherlands.

Blair, C.A., 2000. Modeling three-dimensional thermohaline-driven circulation in the Arabian Gulf. In: Spaulding, M.L., Butler, H.L. (Eds.), Proceedings of the sixth international conference on Estuarine and Coastal Modeling, American Society of Civil Engineers, 74-93.

Elhakeem, A.A., Elshorbagy, W., Chebbi, R., 2007, Oil spill simulation and validation in the Arabian (Persian) Gulf with special reference to the UAE coast, Water Air and Soil Pollution 184, 243-254.

El-Sabh, M.I., Murty, T.S., 1988, Simulation of the Movement and Dispersion of Oil Slicks in the Arabian Gulf, Natural Hazards 1, 197-219.

Elshorbagy, W., Azam, M., Taguchi, K., 2006, Hydrodynamic characterization and modeling of the Arabian Gulf, Journal of Waterway, Port, Coastal and Ocean Engineering, 132 (1), 47-56.

Komen, G.J., Cavaleri, L.; Donelan, M.; Hasselmann, K., Hasselmann, S., Janssen, P.A.E.M., 1995, Dynamics and modeling of ocean waves, Cambridge University Press, Cambridge, UK (page 156).

Korotenko, K.A., Mamedov, R.M., Mooers, C.N.K., 2000, Prediction of the dispersal of oil transport in the Caspian Sea resulting from a continuous release, Spill Science

& Technology Bulletin 6, 323-339.
Lonin, S.A., 1999, Lagrangian model for oil spill diffusion at sea, Spill Science & Technology Bulletin 5, 331-336.
Marinone, S.G., Gonzalez, J.I., Figueroa, J.M., 2009, Prediction of currents and sea surface elevation in the Gulf of California from tidal to seasonal scales, Environmental Modeling & Software 24, 140-143.
MIKE3 User's Guide, Estuarine and coastal hydraulics and oceanography, 2002, DHI Software, DHI Water and Environment, Horsholm, Denmark.
Ommundsen, A., 2002, Models of cross shelf transport introduced by the Lofoten Maelstrom, Continental Shelf Research 22, 93-113.
Pedlosky, J., 1987, Geophysical Fluid Dynamics, 2nd edition, Springer, New York, (pages 75-80).
Pugh, D.T., 1996, Tides, Surges and Mean Sea-Level, John Wiley, New York (page 152).
Rakha, K., Al-Salem, K., Neelamani, S., 2007, Hydrodynamic Atlas for the Arabian Gulf, Journal of Coastal Research SI50, 550-554.
Sabbagh-Yazdi, S.R., 2006, Coupled solution of oil slick and depth-averaged tidal currents on three-dimensional geometry of Persian Gulf, Int. J. Environ. Sci. Tech. 2 (4), 309-317.
Venkatesh, S., 1988, The oil spill behaviour model of the Canadian Atmospheric Environment Service, Part I: Theory and model evaluation, Atmosphere-Ocean 26 (1), 93-108.
Venkatesh, S., Murty, T.S., 1994. Numerical simulation of the movement of the 1991 oil spills in the Arabian Gulf, Water, Air and Soil Pollution 74, 211-234.
Wang, S.D., Shen, Y.M., Zheng, Y.H., 2005, Two-dimensional numerical simulation for transport and fate of oil spills in seas, Ocean Engineering 32, 1556-1571.
Zheng, L., Yapa, P.D., 2000, Buoyant velocity of spherical and non-spherical bubbles/droplets, Journal of Hydraulic Engineering 126 (11), 852-854.
Yanagi, T., Takao, T., 1998, Clockwise phase propagation of semi-diurnal tides in the Gulf of Thailand, Journal of Oceanography 54, pp. 143-150.

Table 1: Specifying the periods and wave numbers of the main constituents

	M_2	S_2	K_1	O_1
T [hr]	12.42	12.00	23.93	25.85
$k \times 10^6$ $[m^{-1}]$	7.58	7.85	3.94	3.64

Table 2: Specifying the phase and amplitude of main constituents for the Kish Island

constituents	M_2	S_2	K_1	O_1
θ : *ph.* [deg]	35.30	69.70	145.31	99.07
μ : *amp.* [*m*]	0.350	0.140	0.333	0.200

Table 3: Comparison of tidal constituents for 4 locations in the Persian Gulf

Tidal constituents	M_2		S_2		K_1		O_1	
	Ph	Amp.	Ph.	Amp.	Ph.	Amp.	Ph.	Amp.
Max. deviation %	15.2	14.1	21.1	27.5	19.8	18.4	20.7	23.4
Min. deviation %	0.6	0.0	1.3	3.6	0.9	1.8	2.9	2.9

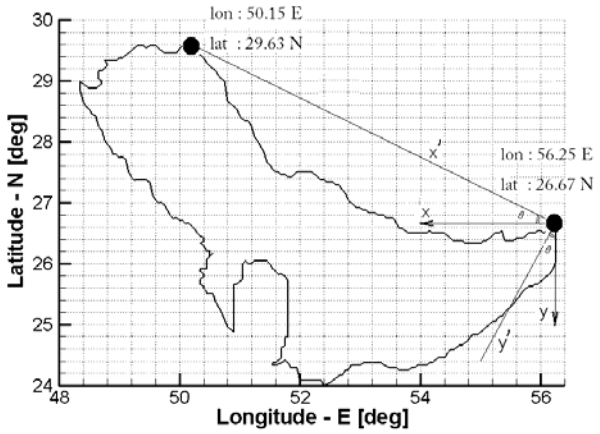

Figure 1: Rotation of the plane of the domain.

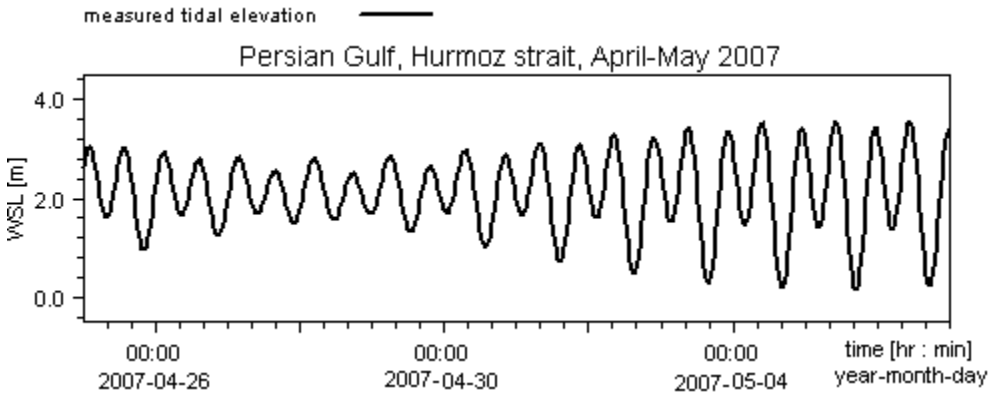

Figure 2: Surface level fluctuations at Didimar Island, imposed at Hurmoz strait.

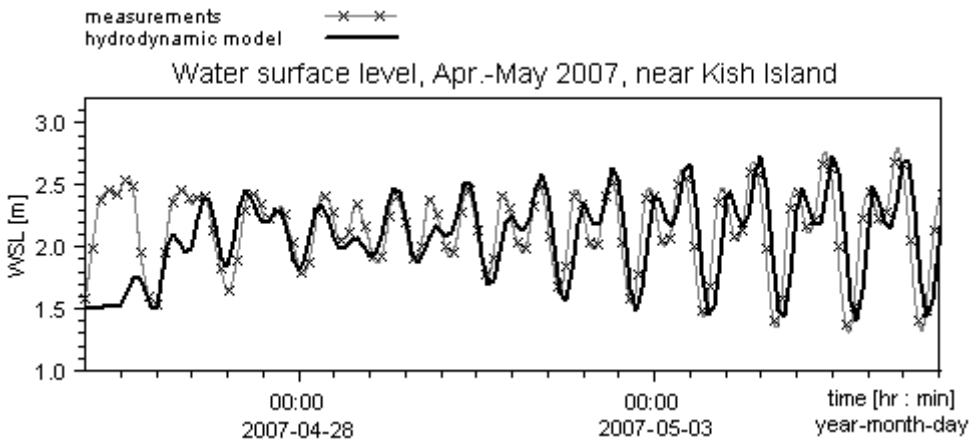

Figure 3: Comparison of computed and measured surface level near Kish Island.

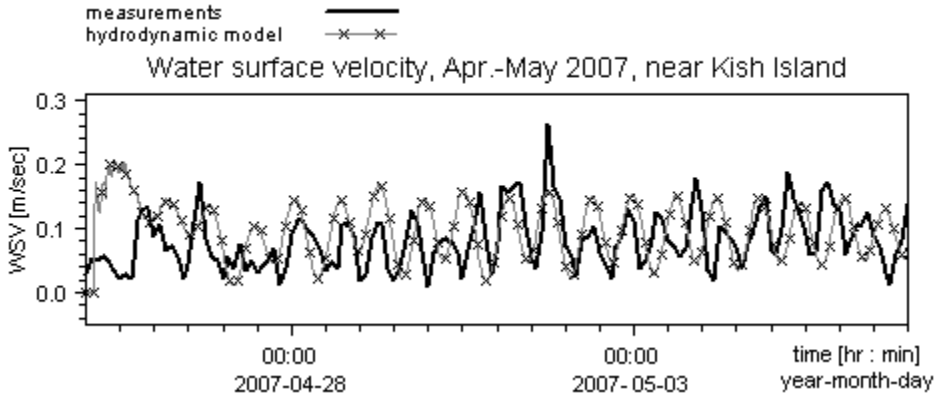

Figure 4: Comparison of computed and measured surface velocity near Kish Island.

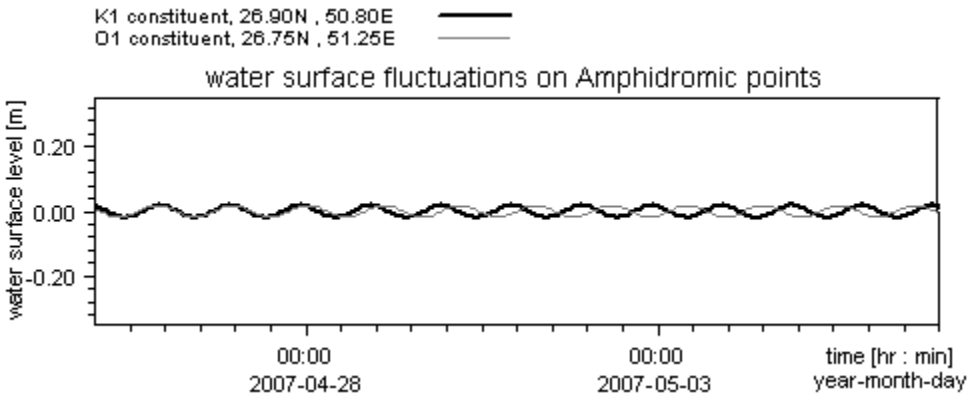

Figure 5: Comparison of surface fluctuations at amphidromic points for K_1, O_1.

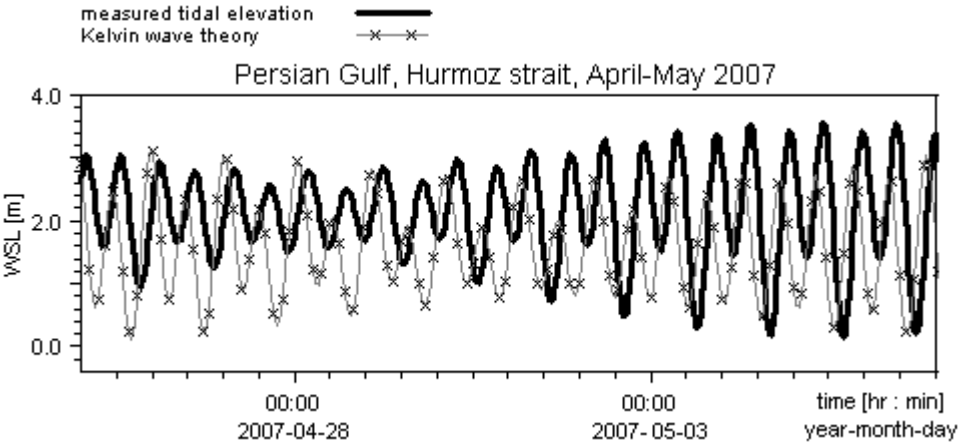

Figure 6: Computed and measured tidal elevation at Didimar Island.

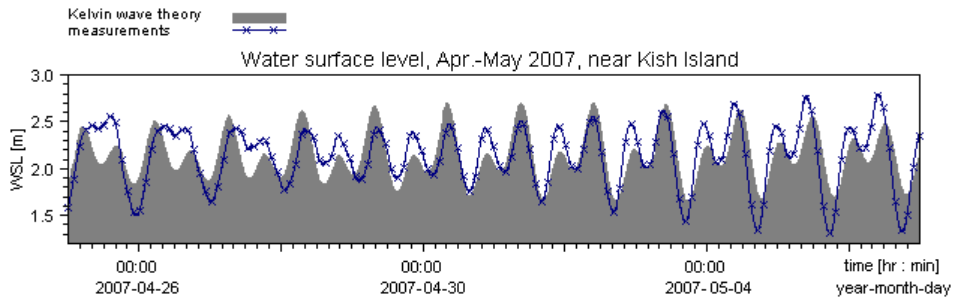

Figure 7: Measured and computed surface level at Kish Island.

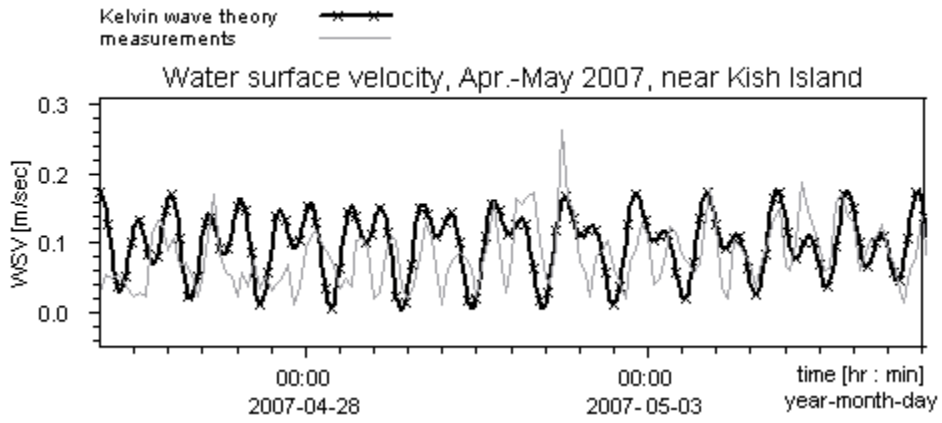

Figure 8: Measured and computed surface velocity at Kish Island.

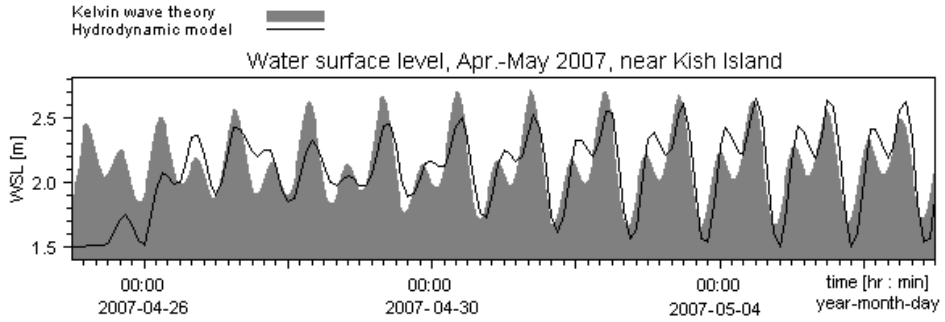

Figure 9: Comparison of WSL near Kish Island for two hydrodynamic models.

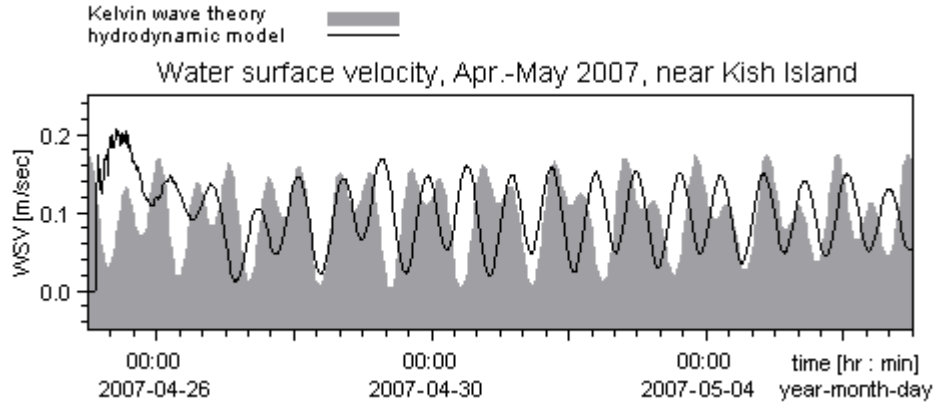

Figure 10: Comparison of WSV near Kish Island for two hydrodynamic models.

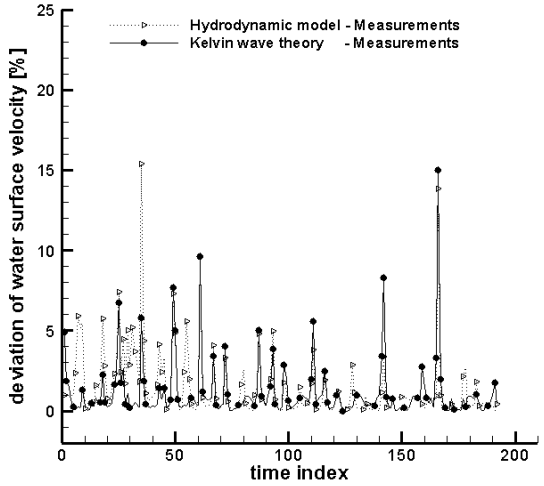

Figure 11: Comparison of surface velocity deviation.

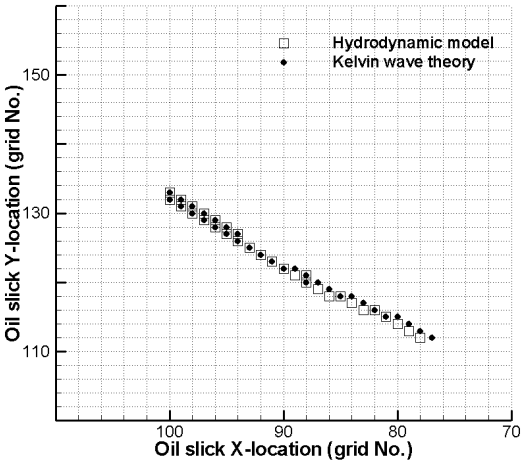

Figure 12: Oil slick location on grid, period of approximately 1.5 days.

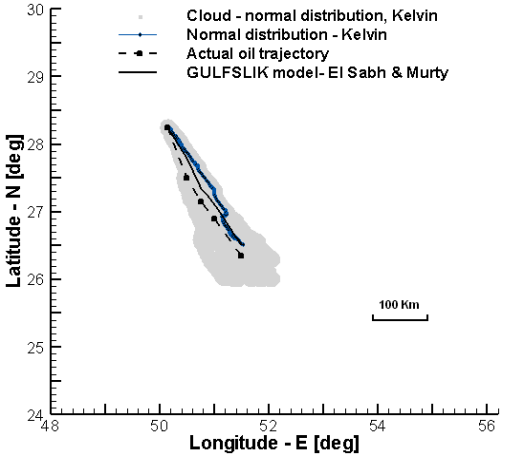

Figure 13: Comparison for the Habash oil spill, period of approximately one week.